Alexandria Engineering Journal (2013) 52, 267–276

Alexandria University

Alexandria Engineering Journal

www.elsevier.com/locate/aej
www.sciencedirect.com

ORIGINAL ARTICLE

# Experimental studies on a DI diesel engine fueled with bioethanol-diesel emulsions

Dulari Hansdah [a,*], S. Murugan [a], L.M. Das [b]

[a] Mechanical Engineering Department, NIT Rourkela, Odisha 769 008, India
[b] Centre for Energy Studies, Indian Institute of Technology, Delhi, India

Received 18 February 2013; revised 20 May 2013; accepted 4 June 2013
Available online 1 July 2013

KEYWORDS

Madhuca Indica flower;
Bioethanol;
Diesel engine;
Combustion;
Performance;
Emission

**Abstract** This paper explores the possibility of utilizing bioethanol obtained from Madhuca Indica flower as an alternative fuel in a direct injection (DI) diesel engine. Three different percentages of bioethanol (5%, 10%, and 15%) on volume basis were emulsified with diesel proportionality with the help of a surfactant. The emulsions were designated as BMDE5, BMDE10, and BMDE15 where the numeric value refers to the percentage of bioethanol. The emulsions were tested as fuels in a single cylinder, four stroke, and air cooled DI diesel engine developing a power of 4.4 kW at 1500 rpm. Results indicated that the bioethanol–diesel emulsions exhibited a longer ignition delay by about 2.2 °CA than that of diesel operation at full load. Overall, the nitric oxide (NO) and smoke emissions were found to be lesser by about 4% and 20%, respectively, with the bioethanol–diesel emulsions compared to that of diesel operation at full load. The BMDE5 emulsion gave a better performance and lower emissions compared to that of BMDE10 and BMDE15. It is suggested that the bioethanol produced from Madhuca Indica flower can be used as a potential alternative fuel replacing 5% of petroleum diesel.



## 1. Introduction

The gap between energy supply and demand increases exponentially as a result of increased population, improved civilization, and industrialization. The consumption of fossil fuels results in increased fuel prices and reduces the availability. The global warming potential (GWP) and ozone depletion potential (ODP) are also adversely affected by the greenhouse gases emitted from the combustion of fossil fuels, other industrial sources, and wastes. Since the fuel crisis arose in the late 1970s, many countries started investing huge amount of money on deriving alternative fuels for heat and power applications. Focus was emphasized to use alternative fuels particularly in internal combustion (IC) engines as they are used in different sectors which include the following: transportation, agriculture, industry, and power. Biomass derived fuels were found to be potential alternative

* Corresponding author. Tel.: +91 9437601094.
E-mail address: dhansdah@gmail.com (D. Hansdah).
Peer review under responsibility of Faculty of Engineering, Alexandria University.

Production and hosting by Elsevier

1110-0168 © 2013 Production and hosting by Elsevier B.V. on behalf of Faculty of Engineering, Alexandria University.
http://dx.doi.org/10.1016/j.aej.2013.06.001

fuels as they are renewable, largely available, and potential of reducing $CO_2$ emissions. Among the biomass derived fuels, bioethanol is considered to be one of the potential alternative fuels for IC engines. Bioethanol can be produced from simple sugar such as sugar cane, sugar beet, and molasses, or from other carbohydrates that can be converted to sugar, such as starch and cellulose. Starchy feedstocks are corn, maize, potatoes, etc., and cellulosic materials are such as wood, forest residue, agricultural residue, crop residue, etc. [1]. Bioethanol produced from food grains and sugar based vegetables like sugar beet restrict the use of bioethanol production in a large quantity in developing countries, because it results in food crisis. Therefore, researchers started to find appropriate methods to derive bioethanol from non-edible feedstocks such as forest residue, wood residue, stem of plant, etc.

Bioethanol has a high Octane number, and hence, it is directly used in spark ignition (SI) engines. However, compression ignition (CI) engines are preferred more than SI engines because the former gives a higher thermal efficiency and are robust in structure. But, bioethanol cannot be used directly in CI engines, because of its low Cetane number. It can be used either by fuel modification by making solution, blend or emulsion with a high Cetane fuel, or carrying out necessary engine modification such as dual fuel mode and surface ignition. Fuel modification is an easier and cheaper method in comparison with engine modification. Phase separation is a common problem noticed in bioethanol diesel blends or emulsion over a wide range of temperature application, presence of water in bioethanol, and its content [2–8]. In order to use the bioethanol–diesel blends in diesel engines, the stability of the blend or emulsion has to be increased with the help of a surfactant and co-solvent. When the temperature of the blend or emulsion increases, it becomes more stable and the solubility of bioethanol in the diesel increases. Research works on the utilization of bioethanol–diesel blends or emulsions in CI engines have been documented, which are beneficial for the implementation of bioethanol as fuel in CI engines [9].

Exhaust emissions from an automotive diesel engine ran with 10% of anhydrous bioethanol diesel blend without any additive were evaluated and compared with diesel operation in the same engine. It was reported that there was a marginal improvement in the engine efficiency compared to that of diesel, and particulate matter emission was reduced [10]. Investigations were carried out to study the performance and exhaust emissions of a heavy duty DI diesel engine fueled with two different diesel ethanol emulsions. The percentages of ethanol were 5% and 10%, and the percentage of surfactant was 1.5% in the emulsion, which was kept constant for both the emulsion. It was reported that there was a reduction in the smoke, $NO_x$, and CO emissions with the use of ethanol–diesel blends with respect to the diesel at full load. The reduction was found to be higher for the higher percentage of ethanol in the blend. The hydrocarbon emission was found to be increased for the ethanol–diesel blend as compared to that of diesel [11].

The present study is aimed to explore the possibility of producing bioethanol from Madhuca Indica flower which is a forest tree residue and to use it in the form of emulsions with diesel in a DI diesel engine. Three different emulsions varying the percentage of bioethanol from 5% to 15% in steps of 5% on volume basis were used as fuels in a single cylinder, four stroke, air cooled, and direct injection diesel engine. The combustion, performance, and emissions parameters of the diesel engine fueled with bioethanol–diesel emulsions were evaluated, analyzed, and compared with those of diesel operation in the same engine.

## 2. Materials and methods

The feedstock used in this study was Madhuca Indica flower, which was collected from the Madhuca Indica tree. It is a forest tree grown abundantly in the tropical regions of Asia and Australia. The residues from the tree are used for different purposes, such as cattle feed and biomass used in direct combustion. The annual production of Madhuca Indica flowers in India in the year 2006 was estimated to be approximately 48,000 M tonnes [12]. The annual production of Madhuca Indica flower was expected to increase in the future, as the Madhuca Indica seeds are considered as one of the potential feedstocks for the biodiesel production in India. Several researchers have carried out research works on the production of biodiesel from Madhuca Indica oil (Mahua oil) by transesterification process and their utilization in diesel engines [13–17]. Methyl ester, ethyl ester, and butyl ester of Madhuca Indica oil were produced using methanol, ethanol, and butanol as reactants with some acid or base catalyst to accelerate the reaction [18,19]. The fresh Madhuca Indica flowers can be used as a source of bioethanol production [12–20]. The tribal people from different locations in India and Pakistan produce country liquor by the fermentation process. Sujit kumar Mohanty et al. [12] established the production method for bioethanol from the Madhuca Indica flowers by solid-state fermentation. They studied various factors, such as the moisture content, initial pH, and temperature, affecting bioethanol production. Fig. 1 shows the schematic diagram of the bioethanol production process.

In this study, bioethanol was produced from Madhuca Indica flowers by the fermentation process, using saccharomyces cerevisiae. The fresh flowers of Madhuca Indica were collected from the village people, cleaned properly to remove the adhering soil particles, and dried in the sunlight. The yeast (*Saccharomyces cerevisiae*) was cultured on YENB (Yeast Extract Nutrient Broth) having 5% glucose and 1% of yeast extract for 48 h. The Madhuca Indica flowers were pretreated for the extraction of sugars. The flowers of Madhuca Indica and distilled water in a 2:1 ratio were autoclaved, at a pressure of 10 lb/inch$^2$ for 15 min. For the fermentation, starter culture was added at the rate of 10% (v/v) to the Madhuca Indica extract taken in a 1000 ml Erlenmeyer flask, and fermentation was carried out in a batch on laboratory bench at a tempera-

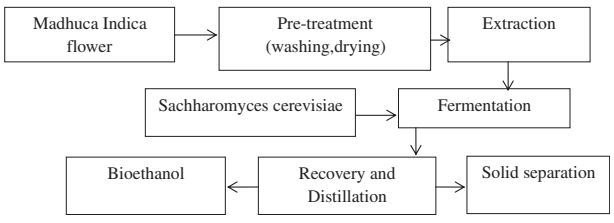


**Figure 1** Production process of bioethanol from Madhuca Indica flower.

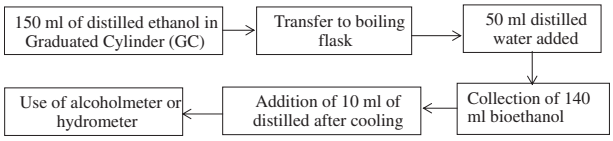


**Figure 2** Layout of checking the purity of bioethanol.

ture of 30 °C ± 2 °C for 96 h. After the fermentation process, first distillation was done to get the crude extract, and further, the fractional distillation was done for the removal of water. The steps involved for checking the purity of bioethanol by an alcoholmeter is shown in Fig. 2.

% of Alcohol = [1.05 ∗ (initial specific gravity – final specific gravity) ∗ 100]/final specific gravity.

**Table 1** Elemental analysis of diesel and bioethanol from Madhuca Indica flower.

| Component | Diesel | Bioethanol from Madhuca Indica flower |
|---|---|---|
| Chemical formula | $C_{10}H_{22}$ | $C_{1.723}H_{4.348}O$ |
| Molecular weight | 144 | 41.024 |
| C wt% | 86 | 54 |
| H wt% | 13.60 | 14.489 |
| N wt% | 0.18 | 0.23 |
| S wt% | 0.40 | 0.717 |
| O wt% | 0 | 38.564 |
| Molar ratio | 6.32 | 3.72 |

**Table 4** Properties of Span 80.

| Properties | Value |
|---|---|
| Chemical name | Sorbitan monooleate |
| Molecular formula | $C_{24}H_{44}O_6$ |
| Molecular weight | 428.6 |
| Density (kg/m$^3$) | 0.995–1.0 5 |
| Saponification value (mgKOH/g) | 140–160 |
| HLB no. | 4.3 |
| Hydroxyl value (mgKOH/g) | 190–220 |
| Acid no. (mgKOH/g) | 8 |
| Iodine value (mg iodine/g) | 60–75 |

## 3. Properties of bioethanol

Table 1 gives the comparison of the ultimate analysis of bioethanol produced from the Madhuca Indica flower with diesel.

Table 2 gives the comparison of physical properties of bioethanol from different feedstocks with Madhuca Indica flower. The properties were tested in a standard fuel testing laboratory, i.e., ITA lab, Kolkata. Also, the comparisons of physical properties of bioethanol emulsions are given in Table 3. The physical properties of Span 80 are given in Table 4. The emulsions of bioethanol and diesel were prepared with 5%, 10%, and 15% of bioethanol and 94%, 89%, and 84% of diesel, respectively, with the addition of a surfactant Span 80 at 1% on volume basis. The surfactant was used to reduce the oil and water surface tension, to make microemulsions by maximizing the surface area. Span 80 has a hydrophilic lipophilic

**Table 2** Comparison of physical properties of bioethanol from different feedstocks with Madhuca Indica flower.

| Properties | ASTM standard | Diesel | B1 [29] | B2 [11] | B3 |
|---|---|---|---|---|---|
| Specific gravity @ 15 °C | D 4052 | 0.863 | 0.790 | 0.78 | 0.80 |
| Lower heating value (MJ/kg) | D 4809 | 43.8 | 26.4 | 26.8 | 29.38 |
| Flash point (°C) | D 2500 | 49 | 22 | 13 | 24 |
| Col filter plugging point (°C) | D 6371 | −19 | Nil | Nil | < −30 |
| Pour point (°C) | D 97 | −15 | −116 | −117 | −103 |
| Boiling point (°C) | D 7169-11 | 180–360 | 78 | 78 | 80 |
| Sulfur content (wt%) | D 093 | 0.049 | 0 | 0 | 0 |
| Bulk modulus of elasticity (bar) | D 6793 | 16,000 | Nil | 13,200 | 13,800 |
| Kinematic viscosity at 40 °C (cSt) | D 445 | 2.58 | 1.36 | 1.35 | 1.73 |
| Moisture content (wt%, wet basis) | Nil | 0.025 | Nil | Nil | 10 |
| Ash (wt%, dry basis) | Nil | 0.13 | Nil | Nil | Nil |
| Carbon residue (%) | D 2500-05 | 0.1 | Nil | Nil | Nil |

*Note*: B1 – bioethanol from sugar molasses, B2 – bioethanol from sugarcane, B3 – bioethanol from Madhuca Indica flower.

**Table 3** Comparison of physical properties of bioethanol emulsions.

| Properties | ASTM standard | BMDE5 | BMDE10 | BMDE15 |
|---|---|---|---|---|
| Specific gravity @ 15 °C | D 4052 | 0.823 | 0.811 | 0.809 |
| Lower heating value (MJ/kg) | D 4809 | 38.21 | 37.02 | 35.34 |
| Kinematic viscosity at 40 °C(cSt) | D 445 | 2.31 | 2.01 | 1.95 |
| Flash point (°C) | D 2500 | 30 | 29 | 26 |
| Cold filter plugging point (°C) | D 6371 | −15 | −20 | −23 |
| Pour point (°C) | D 97 | −9 | −12 | −36 |
| Sulfur content (wt%) | D 093 | 0.012 | 0.007 | 0.002 |
| Boiling point (°C) | D 7169–11 | 165–342 | 142–326 | 114–298 |
| Surface tension at 20 °C (N/m) | D 3825 | 0.016 | 0.019 | 0.02 |

balance (HLB) number of 4.3, and it is more lipophilic than hydrophilic which is an appropriate surfactant for the water-in-oil-emulsion [21]. The resultant mixture was stirred vigorously with the help of a mechanical agitator at the rate of 1800 to 2000 rpm for about 30 min.

The emulsions were kept for an observation for 20 days to check the miscibility. There was no separation found in the emulsion.

## 4. Experimental setup

The investigation was carried out in a single cylinder, four stroke, air cooled, and DI diesel engine which developed a maximum power output of 4.4 kW at constant speed of 1500 rpm. The schematic diagram of the experimental setup is given in Fig. 3. The specifications of the test engine are given in Table 5.

An automatic solenoid controlled type burette is used to measure the fuel consumption. An air box fitted with the engine intake manifold is used to accumulate sufficient air. A manometer fitted in the air box shows the reading of the water head, which is used to calculate the air consumption of the engine. A K-type thermocouple with a temperature indicator fitted in the exhaust pipe indicates the temperature of the exhaust gas. An AVL Digas 444 exhaust gas analyzer shows the measurement of unburnt hydrocarbon (HC), Carbon monoxide (CO), and nitric oxide (NO) emissions when the probe of the analyzer is inserted and kept for a few minutes in the exhaust pipe. The HC, CO, and carbon dioxide ($CO_2$) are measured with the help of the gas analyzer that works on the non-dispersive infrared (NDIR) principle. The nitric oxide (NO) emission is measured by a photochemical sensor. An AVL 437C diesel smoke meter is used to measure the smoke density of the engine exhaust. The cylinder pressure at a particular crank angle is measured with the help of a Kistler made quartz piezoelectric pressure transducer (Model Type 5395A), mounted on the cylinder head in the standard position. A crank angle encoder is fitted to the output shaft to measure the crank angle. The data acquisition system in conjunction with pressure transducer and crank angle encoder will record the pressure and crank angle values. With the help of pressure values obtained for every crank angle degree, the remaining parameters like ignition delay, heat release rate, and combustion duration are calculated with the help of a software and stored in an excel sheet.

**Table 5** Technical specifications of diesel engine.

| Type | Kirloskar TAF1 vertical diesel engine |
|---|---|
| No. of cylinder | 1 |
| Type of injection | Direct |
| Rated power at 1500 rpm (kW) | 4.41 |
| Bore (mm) | 87.5 |
| Stroke (mm) | 110 |
| Compression ratio | 17.5 |
| Method of cooling | Air cooled with radial fan |
| Displacement volume, liters | 0.662 |
| Fuel injection timing BTDC (°) | 23° |
| Number of injector nozzle holes | 3 |

Uncertainty or error analysis is necessary to establish the bounds on the accuracy of the estimated parameters. Evaluations of some unknown uncertainties from known physical quantities were obtained using the following general equation (Coleman and Steele, 1989).

$$\frac{U_Y}{Y} = \left[\sum_{i=1}^{n}\left(\frac{1}{Y}\frac{\partial Y}{\partial xi}U_{xi}\right)^2\right]^{\frac{1}{2}} \quad (1)$$

In the equation cited, $Y$ is the physical parameter that is dependent on the parameters, $xi$. The symbol $U_Y$ denotes the uncertainty in $Y$. By using the above equation, the uncertainty of the experiment was obtained $\pm 3.13\%$. The range, accuracy, and uncertainties of each instrument used in the study are tabulated and given in Table 6.

Initially, the engine was operated with diesel for obtaining the reference data. Then, the experiments were conducted with different percentages of emulsion. For every load, the engine was run with at least 30 min to collect the data for three times. The average of three values of a particular parameter at each load was considered for the analysis.

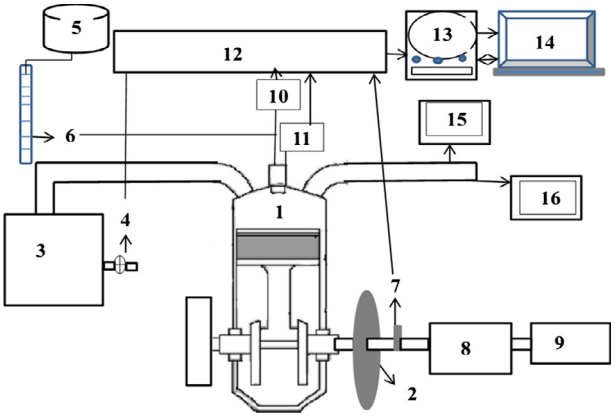


1. Engine
2. Flywheel
3. Air box
4. Manometer
5. Fuel tank
6. Burette
7. Speed sensor
8. Alternator
9. Loads cell
10. Fuel injector
11. Pressure transducer
12. Control panel board
13. Data acquisition card
14. Computer
15. AVL 437C Smoke meter
16. AVL Digas 444 analyser

**Figure 3** Schematic diagram of experimental setup.

**Table 6** Name of instrument and their range, accuracy, and uncertainties.

| Instrument | Range | Accuracy | Percentage uncertainties |
|---|---|---|---|
| Load indicator (W) | 250–6000 | ± 10 | 0.2 |
| Temperature indicator (°C) | 0–900 | ± 1 | 0.15 |
| Speed sensor, (rpm) | 0–10,000 | ± 10 | 1 |
| Burette (cc) | 1–30 | ± 0.2 | 1.5 |
| *Exhaust gas analyzer* | | | |
| NO (ppm) | 0–5000 | ± 50 | 1 |
| HC (ppm) | 0–20,000 | ± 10 | 0.5 |
| CO (% Vol) | 0–10 | ± 0.03 | 1 |
| Smoke meter (%) | 0–100 | ± 1 | 1 |
| Pressure transducer (bar) | 0–110 | ± 1 | 0.15 |
| Crank angle encoder (°CA) | | ± 1 | 0.2 |

## 5. Results and discussion

### 5.1. Combustion parameters

#### 5.1.1. Pressure crank angle diagram

The variation in cylinder pressure with crank angle for the diesel and the three different emulsions is shown in Fig. 4.

It can be observed from the figure that the commencement of ignition for diesel is the earliest, while the commencement of ignition for the BMDE15 emulsion is the latest at full load. The cylinder peak pressures for the BMDE5, BMDE10, and BMDE15 emulsions are 77.07 bar, 76.79 bar, and 77.36 bar, respectively, which is attained approximately at 370.42 °CA, 370.22 °CA, and 371.25 °CA, respectively, at full load, whereas for diesel, it is 73.49 bar at 369.56 °CA. For the BMDE15 emulsion, the combustion pressure occurred approximately about 2 °CA after the diesel ignition. The ignition of the BMDE15 emulsion is the farthest from diesel, while the ignition of the BMDE10 emulsion is the closest to diesel at full load.

#### 5.1.2. Ignition delay

Fig. 5 shows the variation in ignition delay for diesel and bioethanol–diesel emulsions at different loads. The ignition delay is nothing but the time lag between the start of fuel injection and the start of fuel ignition, which is measured in the degree crank angle [22]. It can be observed from the figure that the ignition delay decreases with an increase in the engine load as a result of increased cylinder gas temperature [11]. It is also apparent from the figure that the ignition delay for the bioethanol–diesel emulsions is much longer than that of diesel in the entire engine operation. The difference in the ignition delay between diesel and the bioethanol–diesel emulsions at full load is about 1–2 °CA.

At full load, the BMDE15 emulsion shows the longest ignition delay compared to that of diesel. The lower Cetane number of bioethanol–diesel emulsion is the reason for the longer ignition delay at full load [11].

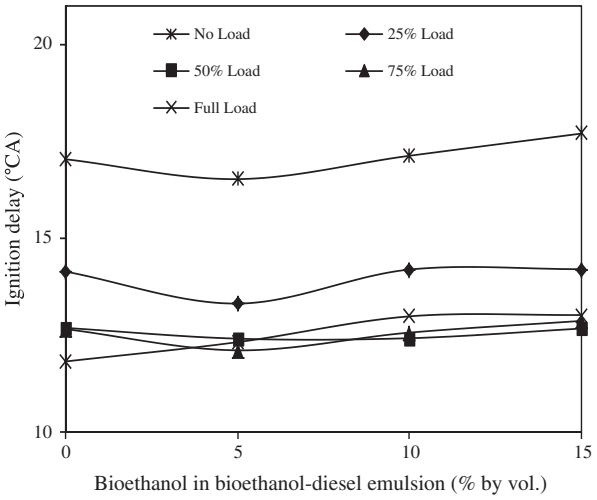


**Figure 5** Variation in ignition delay for diesel and the bioethanol–diesel emulsions at different loads.

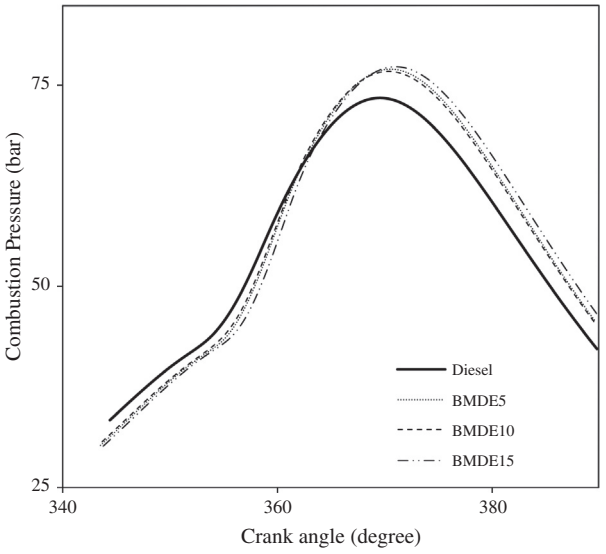


**Figure 4** Variation in cylinder pressure with crank angle.

#### 5.1.3. Heat Release Rate (HRR)

The heat release analysis can provide information about the effects of engine design changes, fuel injection system, fuel type, and engine operating conditions, on the combustion process and engine performance [23]. The heat release rate was calculated by making analysis of the first law of thermodynamics. Sorenson et al. presented the following equation for heat release [24]:

$$\frac{\partial E}{\partial \theta} = \vartheta \frac{\partial P}{\partial \theta}(1/\gamma - 1) + P\frac{\partial \vartheta}{\partial \theta}(1/\gamma - 1) - \frac{\partial \mathrm{E}_w}{\partial \theta} \quad (2)$$

where $\frac{\partial E}{\partial \theta}$ = rate of heat release (J/°CA), $\vartheta$ = gas volume ($m^3$), $P$ = cylinder pressure (bar), $\theta$ = crank angle (°), $\gamma$ = ratio of specific heat, $\frac{\partial E_w}{\partial \theta}$ = rate of heat transfer from the wall (J/°CA).

Fig. 6 illustrates the variation in the heat release rate with the crank angle for diesel and the bioethanol–diesel emulsions at full load. It can be observed from the figure that the maximum HRR is found to be the highest for the BMDE15 emulsion followed by the BMDE5, BMDE10 emulsion and diesel.

In case of the bioethanol–diesel emulsion, more fuel is accumulated in the delay period, and hence, higher HRR is recorded. Another reason may be due to better mixing and complete combustion of the fuel–air mixture. In the case of the BMDE10, the latent heat of vaporization of the emulsion may dominate the other fuel properties, and hence, a lower heat release rate is noticed.

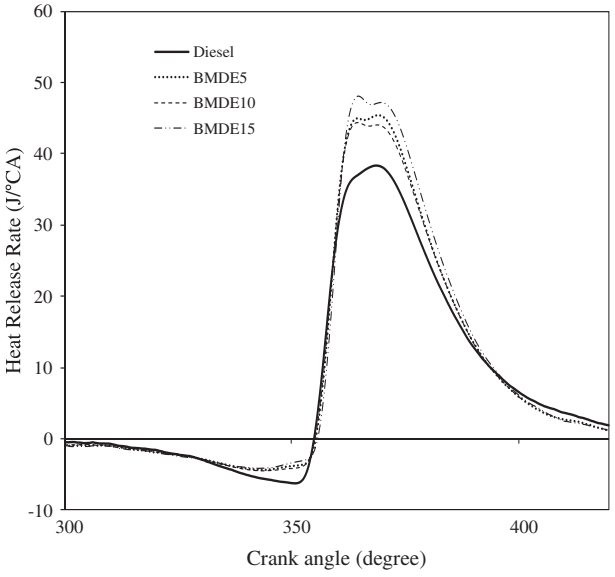


**Figure 6** Variation in heat release rate for diesel and bioethanol–diesel emulsions at different crank angle.

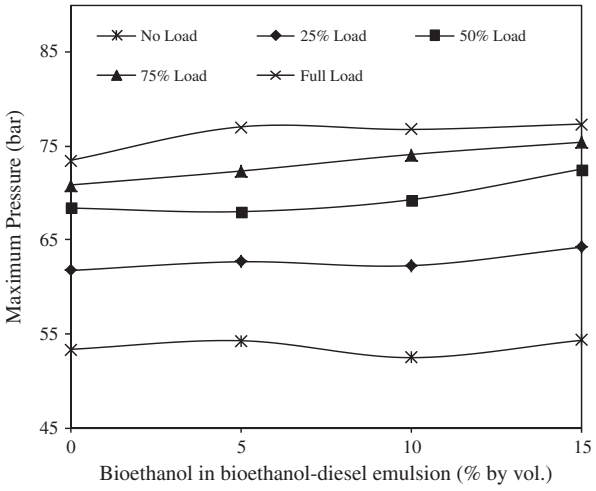


**Figure 7** Variation in maximum pressure for diesel and the bioethanol–diesel emulsions at different loads.

### 5.1.4. Maximum cylinder pressure

Fig. 7 portrays the cylinder pressure for different percentages of bioethanol in the emulsions at different loads. The cylinder peak pressure of a compression ignition (CI) engine is mainly due to the amount of fuel accumulated in the delay period and the combustion rate in the initial stages of premixed combustion. It is evident from Fig. 7 that the maximum cylinder pressures for the bioethanol–diesel emulsions are found to be higher than that of diesel operation, as a result of higher heat release rates. The maximum cylinder pressure for diesel varies from 53.35 bar to 73.49 bar and from no load to full load, respectively. For the BMDE5 emulsion, the values of maximum cylinder pressure from no load to full load are 54.27–77.01 bar, respectively.

In the case of the BMDE10 and BMDE15 emulsions, the maximum pressures are found to be in the range of 52.46–76.79 bar and 54.31–77.36 bar at no load to full load, respectively. The percentage increase in the maximum cylinder pressure for the BMDE5, BMDE10, and BMDE15 emulsions are 3.29%, 2.71%, and 3.78%, respectively, compared to that of diesel at full load.

### 5.1.5. Combustion duration

Fig. 8 shows the combustion duration with respect to the percentage of the bioethanol in the emulsions at different loads. Combustion duration was calculated from the cumulative heat release data computed from the heat release rate, and the duration of 90% of heat release is taken as the combustion duration [25]. The combustion duration decreases with an increase in the bioethanol. The addition of bioethanol with diesel decreases the heating value of the emulsion. On the other hand, the oxygenated fuel can promote the combustion rate, especially the diffusive combustion rate. It can be observed from the figure that at full load, all the bioethanol–diesel emulsions have shorter combustion durations compared to that of diesel.

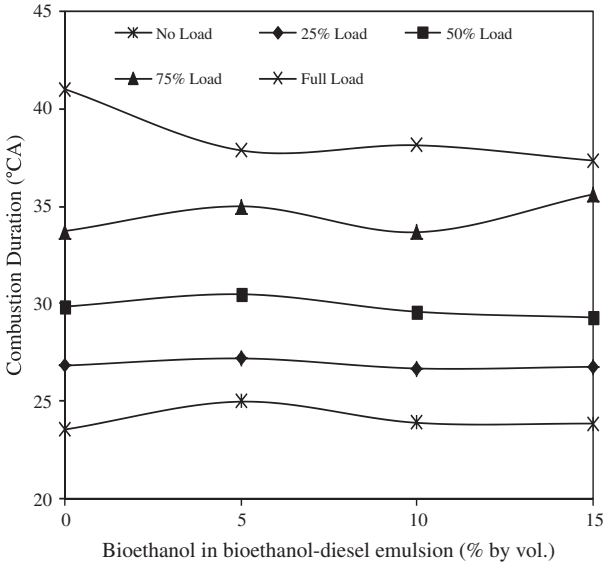


**Figure 8** Variation in combustion duration for diesel and the bioethanol–diesel emulsions at different loads.

The reason may be the faster combustion rate due to high temperature as a result of longer ignition delay and oxygen enhanced combustion [26].

### 5.2. Engine performance analysis

#### 5.2.1. Brake Specific Energy Consumption (BSEC)

Fig. 9 illustrates the variation in the brake specific energy consumption of diesel and bioethanol–diesel emulsions at different loads. The fuel consumption characteristics of an engine are generally expressed in terms of the specific energy consumption in MJ/kW h. If two different fuels of different density and calorific values are blended, then the brake specific energy consumption is considered, instead of the BSFC. It can be observed from the figure that the BSEC decreases with an increase in the brake power. It can also be noticed from the figure that the BSEC for the BMDE5, BMDE10, and BMDE15 emulsions is found to be higher by about 17.26%, 17.5%, and 30.12%, respectively, than that of diesel at full load.

This may be due to the lowering of the energy content of the emulsions caused by the presence of water.

#### 5.2.2. Exhaust Gas Temperature (EGT)

The variation in the exhaust gas temperature with respect to different percentages of bioethanol in bioethanol–diesel emulsions at different loads is shown in Fig. 10. It can be observed from the figure that the exhaust gas temperature increases with increase in load for all tested fuels. The exhaust gas temperature for diesel, BMDE5, BMDE10, and BMDE15 is 315.3, 321.6, 325.6, and 328.2 °C, respectively, at full load. BMDE5 has a lower exhaust gas temperature compared to that of BMDE10 and BMDE15 throughout the entire load operation. This may be due to effective combustion which is taking place in the early stages of exhaust stroke, and hence, there is a saving with respect to exhaust gas energy loss. The BMDE15 possess higher exhaust gas temperature compared to that of diesel, BMDE5 and BMDE10 at full load. The reason may be due to more energy consumption and shorter combustion duration of BMDE15 emulsion [27].

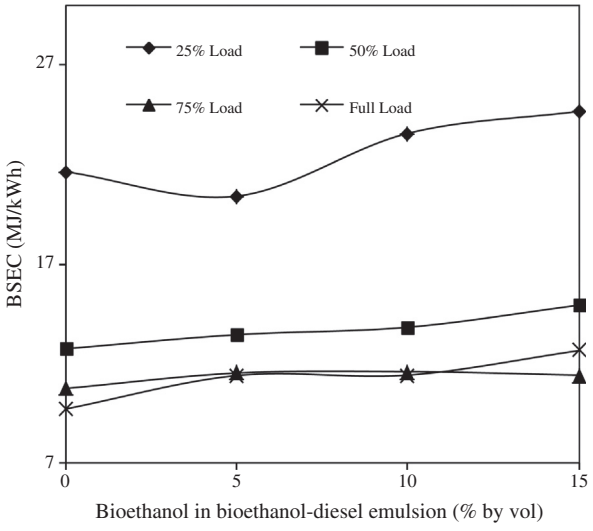


**Figure 9** Variation in BSEC for diesel and the bioethanol–diesel emulsions at different loads.

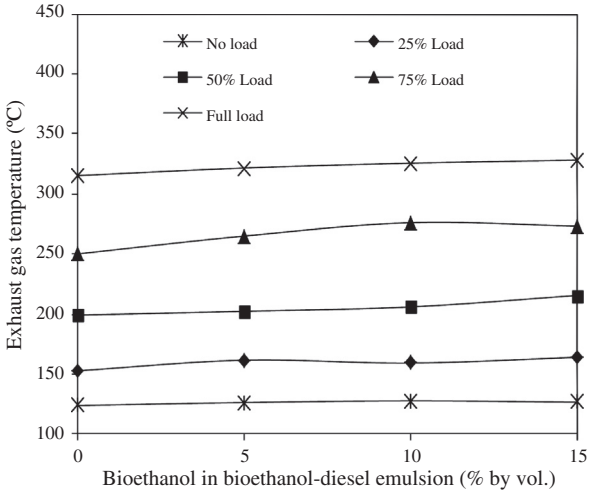


**Figure 10** Variation in EGT for diesel and the bioethanol–diesel emulsions at different loads.

#### 5.2.3. Thermal energy balance

Thermal energy balance is defined as the heat input given by fuel in respect of useful work, heat loss through the exhaust, heat carried away by the lubricating oil, and unaccounted losses (radiation, vapor in the exhaust, heat transfer through fins, etc.). The variation in thermal energy balance for diesel and bioethanol–diesel emulsions at different loads is shown in Fig. 11. Thermal energy balance can be calculated using following equation:

Heat supplied by the fuel is given as:

$$Q = CV^{*}M_f \quad (\text{kJ/h}) \tag{3}$$

where $CV$ = calorific value (kJ/kg), $M_f$ = Mass of fuel consumption (kg/h).

Heat converted to useful work (or) brake work is given as:

$$\text{Useful work (q1)} = \text{Brake power}^{*}3600 \quad (\text{kJ/h}) \tag{4}$$

Percentage of useful work = (useful work/$Q$) * 100.

Heat loss through the exhaust ($q_2$) is given as:

$$q_2 = (Ma + M_f)^{*} C^{*}_{pg}(T_g - T_a) \quad (\text{kJ/h}) \tag{5}$$

where $Ma$ = mass of air consumption (kg/h), $C_{pg}$ = specific heat of gas at different exhaust temperatures (kJ/kg °C), $T_g$ = exhaust gas temperature (°C), and $T_a$ = atmospheric temperature (30 °C)

Heat carried away by the lubricating oil ($q_3$) is calculated as:

$$q_3 = M^{*}_{\text{oil}} C^{*}_{\text{oil}}(T_f - T_i) \quad (\text{kJ/h}) \tag{6}$$

where $M_{\text{oil}}$ = mass flow rate of lubricating oil (kg/h), =(Volume of oil * density of oil)/3600, $C_{\text{oil}}$ = Specific heat of oil at mean average temperature (kJ/kg °C), $(T_f - T_i)$ = temperature rise in oil (°C).

Unaccounted heat loss is given as:

$$q_4 = Q - (q_1 + q_2 + q_3) \quad (\text{kJ/h}) \tag{7}$$

From the graph, it is evident that the useful work increases as the load increased, but other losses are decreased. The useful work for the BMDE5, BMDE10, and BMDE15 emulsions is found to be higher by about 3%, 4%, and 6%, respectively

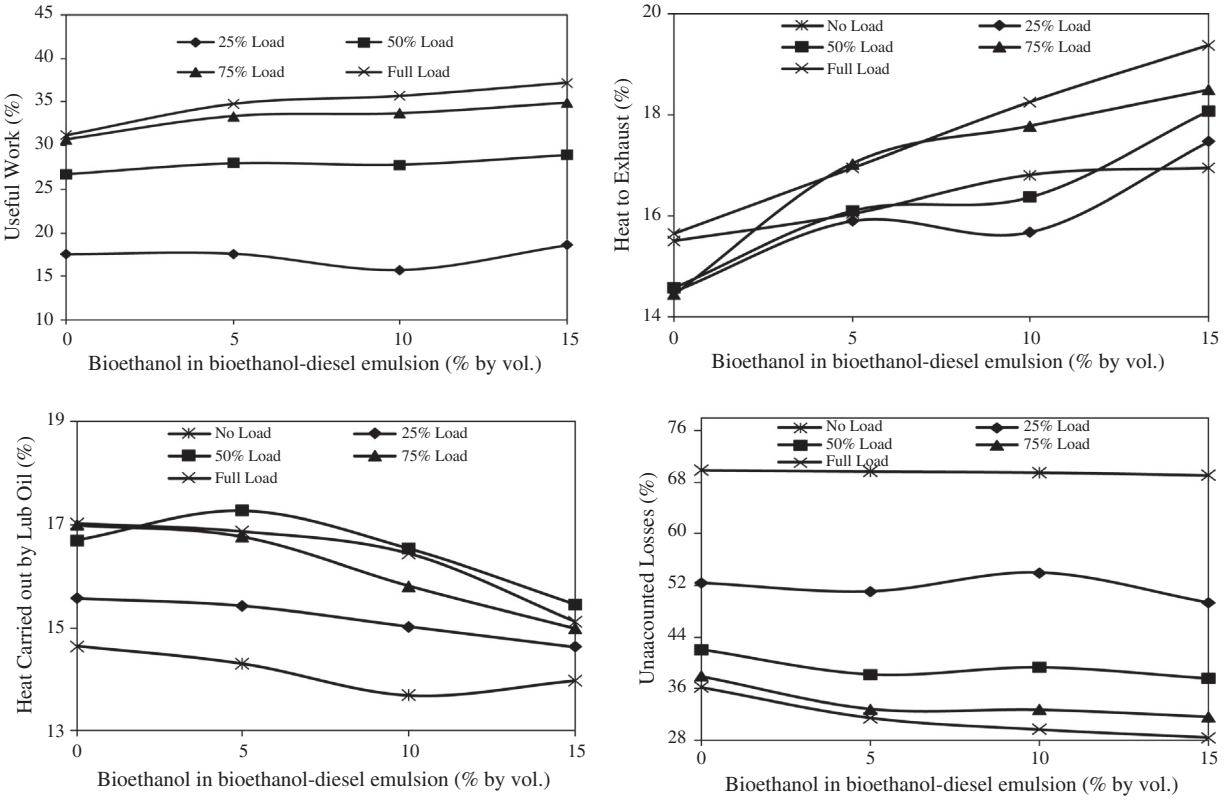


**Figure 11** Variation in thermal energy balance for diesel and the bioethanol–diesel emulsions at different loads.

**Table 7** Thermal energy balance at full load for diesel and bioethanol–diesel emulsions.

| In percentage (%) | Diesel | BMDE5 | BMDE10 | BMDE15 |
|---|---|---|---|---|
| Useful work | 31.1907 | 34.7774 | 35.69706 | 37.21882 |
| Heat to exhaust | 15.6414 | 16.94 | 18.2545 | 19.37857 |
| Heat carried by lubricating oil | 17.02 | 16.863 | 16.436 | 15.12 |
| Unaccounted losses | 36.1479 | 31.4196 | 29.61244 | 28.37736 |

compared to that of diesel at full load. This may be due to efficient combustion of emulsion and cooling effect of bioethanol. Similar result has been reported by Ajav et al. [28].

At full load, the heat loss through the exhaust is found to be higher for all the emulsions compared to that of diesel. Though there is an efficient work is achieved by the emulsions, some amount of heat is lost, may be due to the burning of fuels at the end of expansion stroke. Other losses are minimized with higher percentage of bioethanol operation (Table 7).

### *5.3. Engine emission analysis*

#### *5.3.1. Brake Specific Hydrocarbon (BSHC) emission*

Fig. 12 shows the variation in the BSHC emissions with respect to different percentages of bioethanol in bioethanol–diesel emulsions at different loads.

It can be observed that the BSHC emissions of the three emulsions are found to be higher than that of diesel at full load. The BSHC emissions of BMDE10 and BMDE15 are found to be higher by about 8.33% and 22.16%, compared

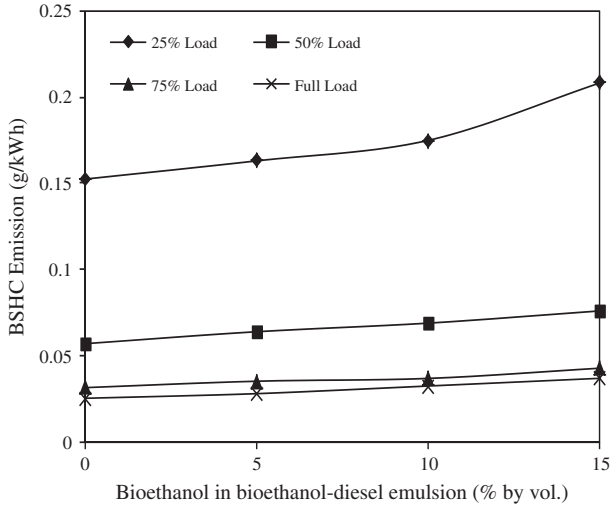


**Figure 12** Variation in BSHC for the diesel and the bioethanol–diesel emulsions at different loads.

to that of diesel at full load. This may be due to the fact that the increase in the volume of bioethanol increases the heat of evaporation and formation of a quench layer. This might slow down the vaporization and mixing of fuel with air, and hence, the BSHC emissions for a given power output increased with an increase in the percentage of bioethanol in the emulsions [29]. The BSHC values of diesel, BMDE5, BMDE10, and BMDE15 at full load are recorded as 0.025, 0.0279, 0.0323, and 0.0368 g/kWh, respectively, at full load.

### 5.3.2. Brake Specific Nitric Oxide (BSNO) emission

The two principal factors that affect the formation of NO emission in a CI engine are the cylinder gas temperature and oxygen availability for combustion [22]. The variation in the BSNO emission given in g/kWh with respect to different percentages of bioethanol at different loads is shown in Fig. 13. It can be depicted from the figure that for BMDE15, the BSNO emission decreases with the increase in the percentage of bioethanol in the emulsion at full load, as a result of high latent heat of vaporization.

However, the BMDE5 and BMDE10 emulsions exhibit lower BSNO emissions compared to those of diesel and the BMDE15 emulsion at part loads. The BSNO emissions for the bioethanol–diesel emulsions are found to be lower than that of diesel throughout the engine operation [29]. The reduction of BSNO in percentage for the BMDE5, BMDE10, and BMDE15 emulsions with respect to diesel at full load is 3.3%, 3.8%, and 4.1%, respectively.

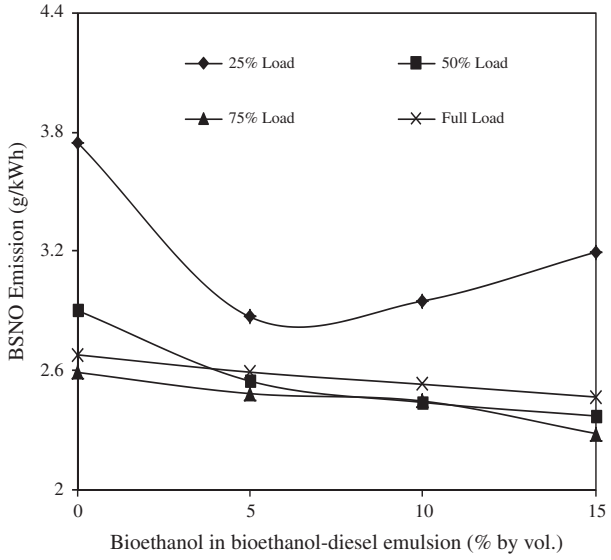


**Figure 13** Variation in BSNO for the diesel and the bioethanol–diesel emulsions at different loads.

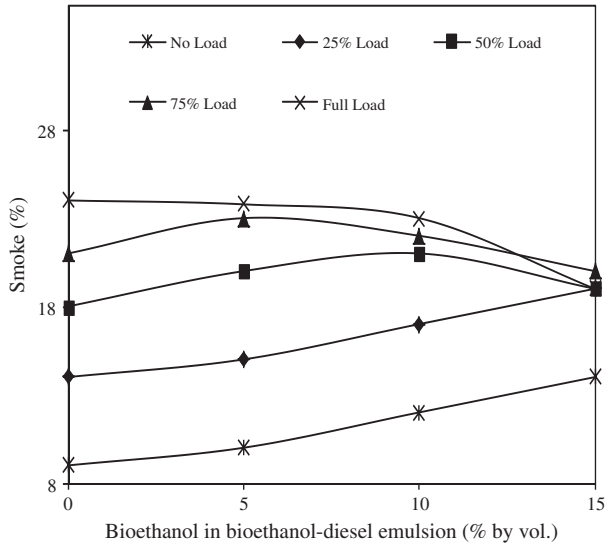


**Figure 14** Variation in smoke for the diesel and the bioethanol–diesel emulsions at different loads.

### 5.3.3. Smoke emissions

Fig. 14 portrays the smoke density for different percentages of bioethanol in the bioethanol–diesel emulsions at different loads. The bioethanol has less number of carbon atoms in it, and hence, the ratio of carbon to hydrogen is two. As a result, lower smoke emissions are recorded for the bioethanol–diesel emulsions.

The smoke emissions of the BMDE5, BMDE10, and BMDE15 emulsions are found to be lesser by about 2.31%, 4.8%, and 20.8%, respectively, compared to that of diesel at full load.

## 6. Conclusion

Experiments have been conducted on a diesel engine using three different bioethanol–diesel emulsions varying the bioethanol fraction by about 5%, 10%, and 15% in the emulsion.

The conclusions of the investigation are as follows:

- The ignition delay of the bioethanol–diesel emulsions is longer by about 1.12, 1.92, and 2.15 °CA, respectively, compared to that of diesel data at full load.
- The maximum cylinder pressures of the BMDE5, BMDE10, and BMDE15 emulsions are higher by about 3.58%, 3.1%, and 3.87%, respectively, compared to that of diesel at full load.
- The useful work for BMDE5, BMDE10, and BMDE15 is higher by about 3%, 4%, and 6%, respectively compared to that of diesel. Heat loss through the exhaust is higher for bioethanol–diesel operation.
- At full load, the HC emission for the BMDE10 and BMDE15 emulsions are higher by about 8.33% and 22.16%, respectively compared to that of diesel, and for BMDE5, the HC emission was found to be lesser by about 5.92% than that of diesel.
- The NO emission for the BMDE5, BMDE10, and BMDE15 emulsions are lesser by about 3.3%, 3.8%, and 4.1%, respectively, in comparison with diesel at full load.
- In comparison with diesel, the smoke emissions of BMDE5, BMDE10, and BMDE15 are lesser by about 2.31%, 4.8%, and 20.8%, respectively, at full load.

## References

[1] A. Demirbas, Bioethanol from cellulosic materials: a renewable motor fuel from biomass, Energy Sour. 27 (4) (2012) 327–337.

[2] P. Satge de Caro, Z. Mouloungui, G. Vaitilingom, J.C. Berge, Interest of combining an additive with diesel and ethanol blends for use in diesel engines, Fuel 80 (2001) 565–574.
[3] P. Kwanchareon, A. Luengnarunumitchai, S. Jai-In, Solubility of a diesel–biodiesel ethanol blend, its fuel properties, and its emission characteristics from diesel engine, Fuel 86 (2007) 1053–1061.
[4] T.M. Letcher, Diesel blends for diesel engines, S. Afric. J. Sci. 79 (1) (1983) 4–7.
[5] J. Lei, L. Shen, Y. Bi, H. Chen, A novel emulsifier for ethanol–diesel blends and its effect on performance and emissions of diesel engine, Fuel 93 (2012) 305–311.
[6] Y. Di, C.S. Cheung, Z. Huang, Experimental study on particulate emission of a diesel engine fueled with blended ethanol–dodecanol–diesel, J. Aerosol Sci. 40 (2) (2009) 101–112.
[7] K.R. Gerdes, G.J. Suppes, Miscibility of ethanol in diesels, Ind. Eng. Chem. Res. 40 (3) (2001) 949–956.
[8] A.C. Hansen, Q. Zhang, W.L. Lyne, Peter ethanol–diesel blends – a review, Bioresour. Technol. 96 (2005) 277–285.
[9] M. Lapuerta, O. Armas, R. Garcia-Contreras, Stability of diesel–bioethanol blends for used in diesel engines, Fuel 86 (2007) 1351–1357.
[10] M. Lapuerta, O. Armas, J.M. Herreros, Emissions from a diesel–bioethanol blend in an automotive diesel engine, Fuel 87 (2008) 25–31.
[11] D.C. Rakopoulos, C.D. Rakopoulos, E.C. Kakaras, E.G. Giakoumis, Effects of ethanol diesel blends on the performance and exhaust emissions of a heavy duty DI diesel engine, Energy Convers. Manage. 49 (2008) 3155–3162.
[12] S.K. Mohanty, S. Behera, M.R. Swain, R.C. Ray, Bioethanol production from Mahula (*Madhuca latifolia* L.) flowers by solid-state fermentation, Appl. Energy 86 (2009) 640–644.
[13] S. Puhan, N. Vedaraman, V.B. Ram Boppana, G. Sankarnarayanan, K. Jeychandran, Mahua oil (Madhuca Indica seed oil) methyl ester as bio diesel-preparation and emission characteristics, Biomass Bioenergy 28 (2005) 87–93.
[14] S. Puhan, N. Vedaraman, G. Sankarnarayanan, B.V. Ramabrahmam, Performance and emission study of mahua ethyl ester in a four stroke direct injection diesel engine, Renew. Energy 30 (2005) 1269–1278.
[15] S. Godiganur, C.H. Suryanarayana Murthy, R.P. Reddy, 6BTA 5.9 G2-1 Cummins engine performance and emission tests using methyl ester mahua (*Madhuca indica*) oil/diesel blends, Renew. Energy 34 (2009) 2172–2177.
[16] H. Raheman, S.V. Ghadge, Performance of compression ignition engine with mahua (*Madhuca indica*) biodiesel, Fuel 86 (2007) 2568–2573.
[17] H. Raheman, S.V. Ghadge, Performance of diesel engine with biodiesel at varying compression ratio and ignition timing, Fuel 87 (2008) 2659–2666.
[18] S. Puhan, N. Vedaraman, B.V. Ramabrahmam, G. Nagarajan, Mahua (*Madhuca indica*) seed oil: a source of renewable energy in India, J. Sci. Ind. Res. 64 (2005) 890–896.
[19] A. Haiter Lenin, R. Ravi, K. Thyagarajan, Performance characteristics of a diesel engine using mahua biodiesel as alternate fuel, Iran. J. Energy Environ. 4 (2) (2013) 136–141.
[20] M.R. Swain, S. Kar, A.K. Sahoo, R.C. Ray, Ethanol fermentation of mahula (*Madhuca latifolia* L.) flowers using free and immobilized yeast *Saccharomyces cerevisiae*, Microbiol Res 162 (2007) 93–98.
[21] D.H. Qi, H. Chen, C.F. Lee, L.M. Geng, Y.Z. Bian, Experimental studies of a naturally aspirated, DI diesel engine fuelled with ethanol-biodiesel-water micro emulsions, Energy Fuels 24 (2010) 652–663.
[22] V. Ganesan, Internal Combustion Engine, third ed., Mc Graw-Hill Companies, 2008.
[23] J. Ghosel, D. Honnery, Heat release model for the combustion of diesel oil emulsions in DI diesel engines, Appl. Therm. Eng. 25 (2005) 2072–2085.
[24] S. Sorenson, T.K. Hayes, L.D. Savage, Cylinder Pressure Data Acquisition and Heat Release Analysis on a Personal Computer, SAE Paper No. 860029, SAE, Warrendale, PA, 1986.
[25] S. Swami Nathan, J.M. Mallikarjuna, A. Ramesh, An experimental study of the biogas diesel HCCI mode of engine operation, Energy Convers. Manage. 51 (2010) 1347–1353.
[26] G.R. Kannan, R. Anand, Experimental investigation on diesel engine with diestrol–water micro emulsions, Energy 36 (2011) 1680–1687.
[27] N. Yilmaz, T.M. Sanchez, Analysis of operating a diesel engine on biodiesel–ethanol and biodiesel–methanol blends, Energy 46 (1) (2012) 126–129.
[28] E.A. Ajav, B. Singh, T.K. Bhattacharya, Thermal balance of a single cylinder diesel engine operating on alternative fuels, Energy Convers. Manage. 41 (2000) 1533–1541.
[29] P. Shanmugam, V. Sivakumar, G. Sridhar, S. Venkatesh, Performance and exhaust emissions of a diesel engine using hybrid fuel with an ANN, Modern Appl. Sci. 3 (2009) 32–37.